Ocean Engineering 171 (2019) 273–285

Contents lists available at ScienceDirect

Ocean Engineering

journal homepage: www.elsevier.com/locate/oceaneng

Modelling of soil-structure-interaction for flexible caissons for offshore wind turbines

Kristoffer Skjolden Skau[a,b,*], Hans Petter Jostad[a,b], Gudmund Eiksund[b], Hendrik Sturm[a]

[a] Norwegian Geotechnical Institute, NGI, Norway
[b] Norwegian University of Science and Technology, NTNU, Norway

ARTICLE INFO

Keywords:
Offshore wind turbine foundations
Soil-structure interaction
Macro-element
Case specific foundation modelling
Caisson flexibility
Design workflow

ABSTRACT

Published foundation models and procedures for calculation of caisson foundation response typically assume a rigid caisson in deformable soil. However, recent published measurement data from a prototype suction bucket jacket has revealed that the lid flexibility of the caisson foundations significantly influences the dynamic foundation stiffness felt by the jacket legs. This paper investigate this soil-structure-interaction problem and presents a modelling approach for including the effect of caisson flexibility in a macro-element. The macro-element, originally developed by assuming a rigid foundation, was modified by included a stiffness correction and a procedure to account for changes in the elastic coupling between horizontal load and moment due to the caisson flexibility. The modified macro-element successfully re-produced the response to general load paths computed by geotechnical finite element analyses, where the foundation was modelled in detail with structural elements and the surrounding soil was represented by continuum elements. The general principles behind the modification is generic in the sense that it can be implemented in other foundation models.

1. Introduction

Offshore wind energy production is increasing continuously and has become an important part of Europe's energy supply. By the end of 2017, more than 3500 offshore wind turbines have been installed in European waters since 1992 (Offshore Wind, GWEC Global Wind, 2016 report, 2017). The monopile is the dominating foundation solution for *Offshore Wind Turbines* (OWT). However, due to increasing water depth and increasing turbine size in future projects, there is an increasing interest for alternative foundation concepts. One of these is the suction caisson, also termed suction bucket or bucket foundation. The suction caisson can be used in two structural configurations – in a mono-tower support structure or a jacket support structure. The *Suction Bucket Jacket* (SBJ) is typically a three or four-legged jacket structure with a caisson foundation supporting each leg. The suction caisson concept is a proven foundation technology used for many years in the oil and gas industry (Andersen et al., 2005; Bye et al., 1995a; Tjelta, 1995, 2001). It is usually made of steel and consists of a base plate (lid) resting on seabed with steel skirts penetrated into the soil. It is installed by applying under pressure (suction) inside the skirts by pumping out water. The differential pressure over the lid gives an additional downward force, and the seepage flow in high permeable soil potentially reduces the skirt tip resistance during penetration. More details on the suction caisson concept can be found in (Bye et al., 1995b; Houlsby and Byrne, 2000; Sturm, 2017; Tjelta, 2001). Fig. 1 shows an illustration of the SBJ supporting an OWT.

OWT-structures are dynamically sensitive and exposed to loads from waves, wind and blade rotations. Accurate prediction of the foundation response is important in design as it influences the dynamics of the structure. The relative importance of the stiffness components is related to the configuration of the support structure, as illustrated in Fig. 2. The rotational foundation stiffness (around the horizontal axis) is of great importance for mono-caisson support structures since the caisson load is dominated by the overturning moment. The vertical caisson stiffness is more important for caissons supporting jackets, since jackets transfer the overturning moment to vertical load pairs.

Prediction and modelling of foundation response is a classical soil-structure-interaction (SSI) problem where the foundation stiffness felt by the structure above involves both the soil response and the flexibility of the foundation itself. Up to now, the caisson is typically assumed to be rigid in methods of foundation stiffness predictions and in foundation models. However, recent measurements presented in Section 2 reveal that the caisson flexibility, in particular the lid flexibility, influences the total foundation stiffness. This paper focuses on this interaction and demonstrate how the caisson flexibility can be included in a foundation model used in integrated analyses of OWTs.

* Corresponding author. Norwegian University of Science and Technology, NTNU, Norway.
E-mail address: kristoffer.skau@ngi.no (K.S. Skau).

https://doi.org/10.1016/j.oceaneng.2018.10.035
Received 23 December 2017; Received in revised form 11 August 2018; Accepted 23 October 2018

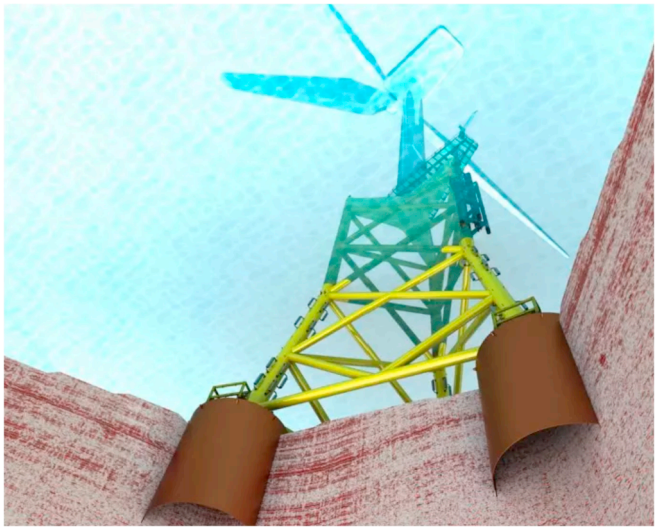

Fig. 1. The Suction Bucket Jacket, an application of the suction bucket concept.

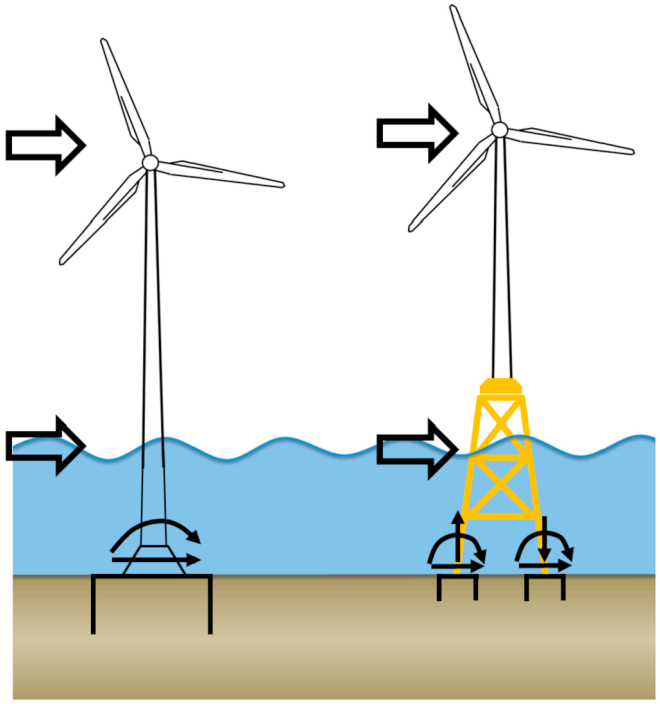

Fig. 2. Loads on caisson foundations supporting a) a mono tower and b) a jacket.

1.1. Organization of paper

This first part of the paper (Section 2-5) presents a literature review of foundation modelling, a discussion on the recent measurement data and, most important, the proposed modelling approach for including flexibility of the caisson in a foundation model. The foundation model considered was the macro-element proposed by (K. S. S. Skau et al., 2018a), which was developed for shallow skirted foundations and caissons. Section 4 gives a brief presentation of the macro-element and Section 5 explains the modification of this macro-element in order to include the effect of flexibility of the caisson.

The second part of the paper (Section 6-8) addresses the effect of caisson flexibility by finite element analyses (FEA) of a defined case. Section 6 compares the macro-element response with the FEA results. Section 7 presents some observations from the FEA supporting the assumptions behind the macro-element modification. Based on these observations, Section 8 presents a 2-step approach of FEA sub-modelling of the caisson flexibility to make the design analysis work flow more efficient.

2. Literature review and field measurements

In design practise and research, it is common and often reasonable to assume suction caissons to be rigid. A typical example is a spudcan at failure. However, structures that intuitively appear nearly rigid may deform significantly and influence the overall response as shown for gravity based structures by (Andresen et al., 2011; Skau et al., 2010). The effect of caisson flexibility seems to be ignored in most research. In published studies and in proposed prediction methods of foundation stiffness, the foundation is typically assumed to be fully rigid (Bordón et al., 2016; Dekker, 2014; Doherty and Deeks, 2003; Suryasentana et al., 2017; Vabbersgaard et al., 2009). Liingaard et al. (2007), Jalbi et al. (2018) and Doherty et al. (2005) studied foundation stiffness assuming flexible skirts but rigid lid. Doherty et al. (2005) suggested correction factors to account for the skirt flexibility, but found it to influence the global stiffness by less than 4% for reasonable skirt thicknesses. Both Liingaard et al. (2007) and Doherty et al. (2005) consider the skirt flexibility to have little impacts on global foundation response compared to other properties such as the soil stiffness and foundation geometry. Strikingly, the effect of lid flexibility has not been addressed in any published prediction method known by the authors. The assumption of a rigid lid may be challenged in OWT design, where foundations are optimized to reduce cost, leading to thin-walled skirts and more slender lid stiffeners.

At the time the presented work was conducted, only a limited number of OWTs using suction caisson foundations were installed. One OWT, installed by DONG Energy, is the Borkum Riffgrund 01 –Suction Bucket Jacket (BKR01-SBJ) in the Germany Bight of the North Sea. The BKR01-SBJ has three legs resting on 8 m diameter buckets (caissons) with an aspect ratio, $h/D = 1.0$, where D is the diameter and h is the skirt length. The ground conditions comprises mainly dense sand intermitted by a few thin silty sand layers. The jacket supports a 4 MW S turbine. BKR01-SBJ is extensively instrumented to measure the in-place behaviour in order to confirm or improve future designs (Shonberg et al., 2017). has summarized several observations made in the period between 2014 and 2016. One aspect discussed by the authors is the effect of lid deflection. They found from the measurements that the lid flexibility significantly affects the total vertical stiffness felt by the jacket leg. This can be seen from the measurements in Fig. 2, showing lid stiffness, soil-skirt stiffness, and total stiffness as interpreted by (Shonberg et al., 2017). The term soil-skirt stiffness ($k_{soil-skirt}$) denotes the load-displacement response of the top of the skirts, the term lid stiffness (k_{lid}) denotes the response of the lid deflection, and the term total stiffness (k_{total}) denoted the combined stiffness as it is felt by the jacket leg. The stiffness values are normalized by $k_{v,ref}$, a random value, to anonymize the measured values. Fig. 2 shows that the measured flexibility from the vertical lid deflection is approximately 50% of the measured mean value of the total foundation flexibility. The observation demonstrates the importance of including the lid stiffness in the calculation of foundation stiffness. Based on the measurements (Shonberg et al., 2017), found that the total vertical foundation stiffness can be modelled as two series-coupled springs:

$$\frac{1}{k_{total}} = \frac{1}{k_{lid}} + \frac{1}{k_{soil-skirt}} \tag{1}$$

The additional caisson flexibility may influence the dynamic behaviour of the structure, thus the fatigue damage during the life time. It will also give additional displacement/rotation that has to be considered when evaluating the SLS requirement of maximum allowable turbine rotation.

3. Foundation modelling by the macro-element approach

As already mentioned, OWT-structures are dynamically sensitive and exposed to loads from waves, wind and blade and rotor excitations. An optimal and safe design depends on analyses that accurately capture the dynamics of the structure. It is therefore recommended to carry out integrated dynamic analyses of the structure in the design of offshore wind turbines (DNV, 2016). State of the art integrated dynamic analysis includes the structure, aerodynamic loads, hydrodynamic loads, pitch controller and foundation/soil reactions. To capture the nonlinear coupling between the loads, it is necessary to run the integrated analyses in time domain. The soil and foundation models in the analyses are unfortunately still relatively simple (e.g. p-y spring elements). However, the macro-element concept is a viable approach for modelling foundation response in integrated analyses. It works as a boundary condition for the OWT-structure in a structure-foundation interface (*SFI*). The macro-element is computational effective compared to a model that represents the soil domain as a continuum, since it does not compute stresses and strains in the soil, but includes the effect of these implicitly in its formulation. This is similar to describing a beam response by changes in moment and curvature rather than stresses and strains in the beam cross sections. Reference is made to (Houlsby, 2016; Houlsby et al., 2005) for a thorough discussion on the conceptual basis of the macro-element.

A macro-element will typically be formulated as a 3 degrees of freedom model (considering vertical load, horizontal load and overturning moment in one plane) or as a 6 degrees of freedom model considering all load directions. To reflect observed foundation behaviour, it is necessary to formulate the models such that the different DOFs are coupled and non-linear. Constitutive models have been the inspiration for most macro-element models as these frameworks are well suited to model foundation behaviour as well as stress-strain relationships. The pioneering work by (Butterfield and Ticof, 1979; Nova and Montrasio, 1991; Roscoe and Schofield, 1956) introduced and formalized the concept of macro-elements for shallow foundations. Recent macro-elements continuously introduce more complex issues such as cyclic loading, soil-structure-gapping and various soil conditions. The models proposed today are also often application oriented considering, e.g. earthquakes (Cremer et al., 2001; Grange et al., 2009; Prisco and Wood, 2012), spudcan for jack-ups (Bienen et al., 2006; Cassidy et al., 2004; Jostad et al., 1994; Martin, 1994; Martin and Houlsby, 2001) and shallow skirted foundations for OWT (Byrne, 2000; Ibsen et al., 2014; Nguyen-Sy and Houlsby, 2005).

The macro-elements available in the literature are based on the assumption of a rigid foundation. To include the effect of foundation flexibility, the existing macro-elements must be modified. In this paper, it was chosen to modify the macro-element presented in (K. S. S. Skau et al., 2018b) to include foundation flexibility. However, the principles behind the modification is relevant for general foundation modelling, and can be implemented in other models as well.

4. Macro-element formulation for a rigid foundation

Before describing the modifications to account for flexibility in the foundation, it was found reasonable to include some key aspects of the original formulation. A more thorough presentation can be found in (K. S. S. Skau et al., 2018a). Fig. 3 shows the nomenclature of the macro-element and the definition of the soil foundation interface (*SFI*). The moment and rotation are expressed as energy conjugates with the same units as the vertical and horizontal loads and displacements. The vectors are written:

$$\boldsymbol{F} = \begin{bmatrix} V \\ H \\ 2M/D \end{bmatrix}, \ \boldsymbol{u} = \begin{bmatrix} u_v \\ u_h \\ u_\theta \cdot D/2 \end{bmatrix} \tag{2}$$

The macro-element is formulated within the framework of multi-surface plasticity and pure kinematic hardening. The multi-surface plasticity approach was developed in the 1950s and 1960s motivated by the need for describing behaviour of metals when subjected to cyclic loading (Iwan, 1967; Prager, 1955; Ziegler, 1959). The principle of multi-surface plasticity is illustrated in Fig. 4, where surfaces translate in a load space, each of them with a plastic contribution to the overall plastic displacement (du^p). This is expressed mathematically by the Koiter rule (Koiter, 1953)(see Fig. 5):

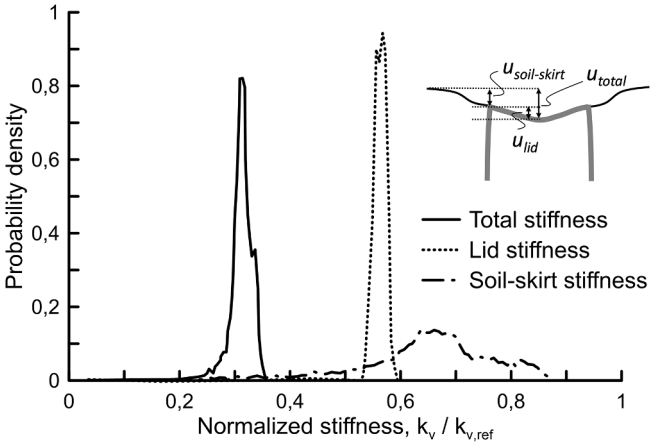

Fig. 3. Total stiffness, lid stiffness and soil-skirt stiffness of a caisson foundation (after Shonberg et al., 2017).

$$du^p = \sum_{i=1}^{k} du_i^{\,p} = \sum_{i=1}^{k} d\lambda_i \cdot \partial g_i \big/ \partial \boldsymbol{F} \tag{3}$$

where k is the outermost surface being violated (or activated). The surface translation for every surface i is expressed by the kinematic hardening vector $\boldsymbol{\alpha}_i$. The hardening law, relating the kinematic hardening parameter and the incremental plastic multiplier ($d\lambda_i$), is based on the soil model proposed by Grimstad et al. (2014) and expressed as:

$$d\boldsymbol{\alpha}_i \big/ d\lambda_i = \boldsymbol{D}_i^p \cdot \partial g_i \big/ \partial \boldsymbol{F} \tag{4}$$

where $\partial g_i / \partial \boldsymbol{F}$ is the plastic flow direction vector, and $\boldsymbol{D}_i^p$ is the plastic stiffness matrix for surface i. The hardening law is similar to The plastic stiffness matrix capture the anisotropic nature of the foundation response. In three dimensions, the matrix is expressed:

$$\boldsymbol{D}_i^p = \begin{bmatrix} k_{i,v}^p & 0 & 0 \\ 0 & k_{i,h}^p & 0 \\ 0 & 0 & k_{i,u_\theta}^p \end{bmatrix} \tag{5}$$

$k_{i,v}^p$, $k_{i,h}^p$, k_{i,u_θ}^p refer to the plastic stiffness in the vertical direction, horizontal direction and rotation around the out of plane axis.

The multiple yield surfaces in the model are defined based on the shape of contours of plastic work at monotonic loading, and the plastic flow direction is defined to be associated, i.e. normal to the yield

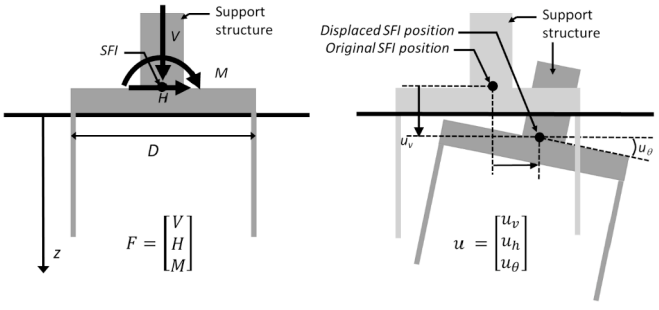

Fig. 4. Nomenclature of the macro-element and definition of the SFI.

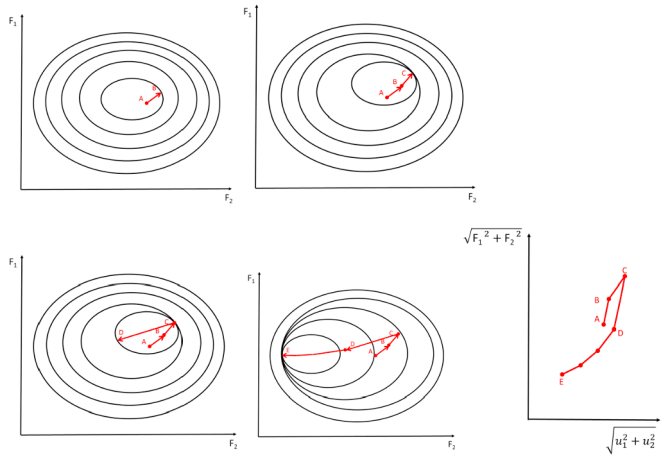

Fig. 5. Illustration of the multi-surface plasticity principle with translation of yield surfaces in the F_1 - F_t load space.

surface. Most macro-elements typically use a rotated yield surface to capture the behaviour under combined moment and horizontal loading. This is based on the asymmetric response observed in model tests and numerical studies, e.g. (Gottardi and Butterfield, 1993; Gourvenec and Barnett, 2011; Martin, 1994; K. S. Skau et al., 2018b). The macro-element proposed by (K. S. S. Skau et al., 2018a) included this effect by defining a load reference point (*LRP*) different from the *SFI*. The *LRP* is a theoretical quantity, defined to obtain a stiffness matrix without any coupling terms between the moment and the horizontal load. For rigid foundations, the *LRP* can be interpreted as the rotation point under pure moment loading. The *LRP* can be calculated approximately as:

$$z_{LRP} = \frac{u_{h,SFI}}{u_\theta} \tag{6}$$

where $u_{h,SFI}$ is the horizontal displacement at the SFI and u_θ is the rotation of the *SFI* when subjected to pure moment load at *SFI*. The depth refers to the distance from the SFI. If the *LRP* is determined based on displacement and rotation at high mobilization, the *LRP* represents a plastic decoupling point, and the yield and potential surfaces can be approximated by ellipses without any rotation to the vertical, horizontal and moment axis, and written:

$$f_i = \left(\frac{V - \alpha_{i,V}}{V_{i,max}}\right)^2 + \left(\frac{H - \alpha_{i,H}}{H_{i,max}}\right)^2 + \left(\frac{M - \alpha_{i,M}}{M_{i,max}}\right)^2 - 1 \tag{7}$$

where the denominators $V_{i,max}$, $H_{i,max}$ and $M_{i,max}$ are the axis crossings for the surface i. $\alpha_{i,V}$, $\alpha_{i,H}$, $\alpha_{i,M}$ are the coordinates of the origin (initially equal zero) of surface i. All values relate to the reference point, z_{LRP}, which has to be specified as an input parameter.

With the assumption of a rigid foundation, it was found reasonable to describe the elastic stiffness matrix at z_{LRP} as a diagonal matrix, thus no coupling between the horizontal displacement and the rotation:

$$\boldsymbol{D}_{z_{LRP}} = \begin{bmatrix} k_v^e & 0 & 0 \\ 0 & k_h^e & 0 \\ 0 & 0 & k_\theta^e \end{bmatrix} \tag{8}$$

The stiffness coefficients k_v, k_h and k_θ refer to the elastic stiffness in vertical, horizontal and rotational direction. The fact that the elastic stiffness matrix is a diagonal matrix, and the yield function describe an ellipse without rotation, implies that the value of z_{LRP} is constant for all load combinations and levels. This approximation was based on a numerical study of skirted foundations in different soil conditions. The approximation limits the required input to the macro-element. As discussed in Section 5, this assumption needs to be revisited when the caisson flexibility is included.

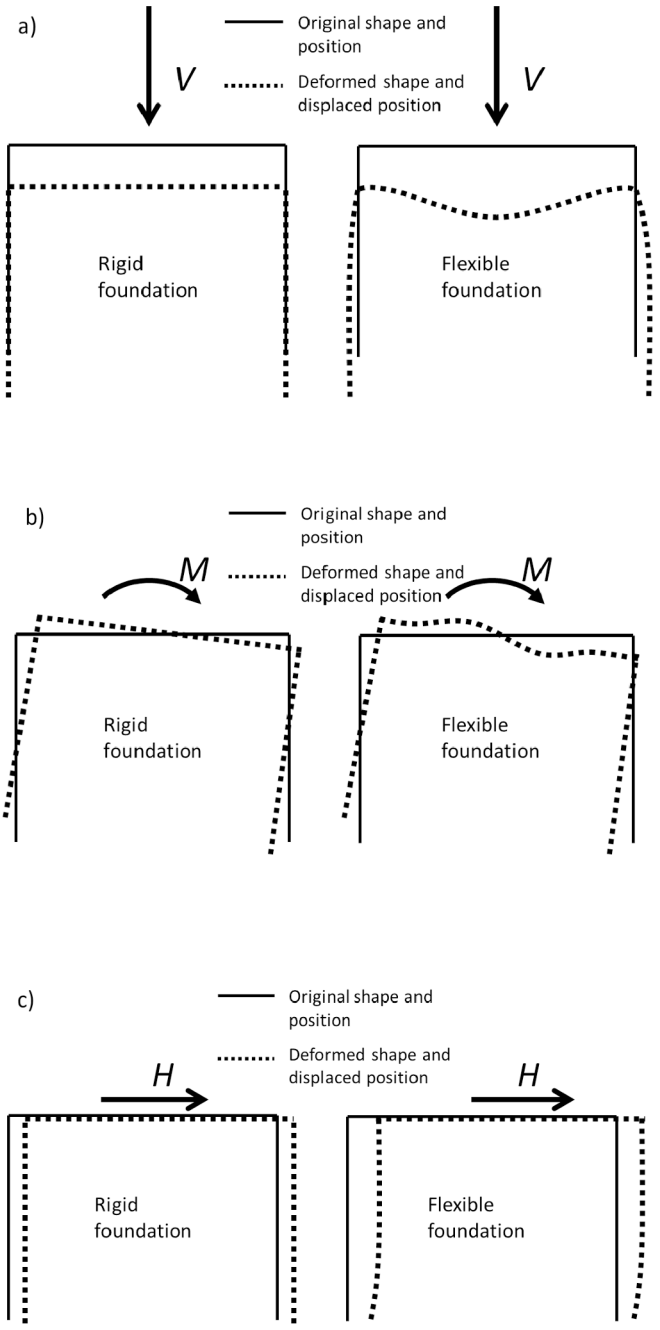

Fig. 6. Foundation deflection mode considered in the study. a) Vertical lid deflection, b) lid bending deflection, c) skirt deflection.

5. Modifications to account for caisson flexibility

5.1. Relevant deformation modes for flexible caissons

The macro-element formulation was modified to account for caisson flexibility on the basis of possible deflection modes. Note that only plate deflection was considered in this work. The length of the skirt and the diameter of the lid were assumed constant. The load was assumed to be applied at the centre of the lid of the caisson. Fig. 6 shows three modes illustrating the difference between a rigid and flexible caisson. These modes define a set of fundamental deflection modes for a flexible caisson foundation. The figures are explained below(see Fig. 7):

a) Vertical deflection of the lid

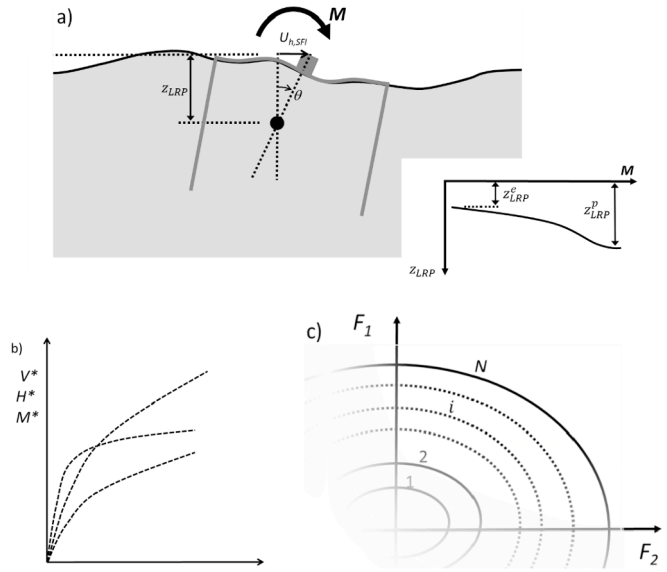

Fig. 7. Illustration of the required model input: a) Depth to load reference points, z^e_{LRP} and z^p_{LRP}, b) Input load-displacement response c) Number of surfaces.

Fig. 6a shows how a vertical load on the flexible caisson will cause a deflection of the lid. The deflection will impose a volume change in the soil plug, thus for undrained conditions, increase the total mean stress. The increased mean stress will give an increased radial stress against the skirt wall, enforcing hoop deformations along the skirt periphery. The vertical lid deflection mode is therefore a combined mode which involves both lid deflection and skirt deflection (hoop deformations).

b) Bending deflection of the lid

Fig. 6b shows how a moment load bends the lid locally. The mode will increase the shear mobilization below the lid, but it will not try to impose a volume change of the skirt compartments and increase the mean stress in the soil plug. The influence zone is therefore relatively limited, and the lid deflection is not coupled to the skirt stiffness, as it is for the vertical deflection mode.

c) Deflection of the skirt.

Fig. 6c shows how a horizontal load bends the skirts. The skirt bending can be a result of shear deformation of the caisson skirt, or an ovalization of the skirt periphery. It should be noted that the load situation illustrated in Fig. 6c is somewhat incomplete, as the figure implicitly assume a restriction of the lid rotation/bending. Without this restriction, the lid can bend, and the deformation mode would have been a combination of the modes in Fig. 6b and c.

The three idealized deformation modes are useful as they give a clear picture of the effects that have to be captured by the macro-element. The proposed modification builds on the deduced consequences of these modes. Firstly, all the modes considered are assumed to influence the soil locally. However, the structural deformations are small compared to the dimensions of the foundation. Thus, a rigid body translation of the deformed and non-deformed shape will imposed approximately the same total soil resistance. Secondly, all loads has to be transferred trough the flexible caisson. This implies that the caisson deformation modes can be modelled as an independent mode, embedded inside the global mode. This is analogue to the 1D series coupled springs model in equation (1) but extended to three degrees of freedom.

Referring to the above discussion, it was decided to modify the macro-element based on the two assumptions:

1) The foundation flexibility can be included as a linear elastic contribution
2) The foundation flexibility can be included as a series coupled stiffness contribution in line with equation (1) but extended to 3 DOF.

The implication of these assumption is that the elastic flexibility matrix of the whole flexible caisson foundation ($\boldsymbol{D}^{-1}_{foundation}$) is given by the sum of the elastic caisson flexibility matrix ($\boldsymbol{D}^{-1}_{flex\ caisson}$) and the flexibility matrix representing the elastic global response assuming a rigid foundation ($\boldsymbol{D}^{-1}_{rigid\ bucket}$):

$$\boldsymbol{D}^{-1}_{rigid\ caisson} + \boldsymbol{D}^{-1}_{flex\ caisson} = \boldsymbol{D}^{-1}_{foundation} \tag{9}$$

Note that it is sufficient to know that the stiffness matrix $\boldsymbol{D}_{foundation}$ exists. It is not necessary to identify the exact contributions from each of the two matrices $\boldsymbol{D}_{rigid\ bucket}$ and $\boldsymbol{D}_{flex\ bucket}$.

It becomes clear from Fig. 6 that the bending of the lid moves the *LRP* closer to the lid when calculated by equation (6). This will give a more pronounced variation in z_{LRP} as function of mobilization, i.e.: the difference between the elastic and plastic *LRP* may become significant. The assumption of a coinciding elastic and plastic point of rotation from (K. S. S. Skau et al., 2018b), is difficult to defend based on this reasoning. However, the two assumptions above enables a relatively simple implementation of the flexibility into the macro-element. The concept of one *LRP* has to be modified and separated into two quantities:

1) Depth of the rotation centre for the elastic response, z^e_{LRP}.
2) Depth of the rotation centre for the plastic response, z^p_{LRP}.

The determination of the two depths are commented upon later. For now, the modification only imply that a diagonal elastic stiffness matrix, $\boldsymbol{D}_{z^e_{LRP}}$, exists at the z^e_{LRP}, expressed as:

$$\boldsymbol{D}_{z^e_{LRP}} = \begin{bmatrix} k^e_v & 0 & 0 \\ 0 & k^e_h & 0 \\ 0 & 0 & k^e_\theta \end{bmatrix} \tag{10}$$

The stiffness coefficients $k_v{}^e$, $k_h{}^e$ and $k_\theta{}^e$ refer to the elastic stiffness in vertical, horizontal and rotational direction at z^e_{LRP}. The model formulation still relies on the yield function and the potential function, described in a coordinate system with the origin at the depth of the plastic rotation point, z^p_{LRP}. Thus, the elastic stiffness matrix is simply transferred to this depth by the coordinate transformation matrix $\boldsymbol{T}$,

$$\boldsymbol{D}_{z^p_{LRP}} = \boldsymbol{T}^T \boldsymbol{D}_{z^e_{LRP}} \boldsymbol{T} \tag{11}$$

where:

$$\boldsymbol{T} = \begin{bmatrix} 1 & 0 & 0 \\ 0 & 1 & -(z^p_{LRP} - z^e_{LRP}) \\ 0 & 0 & 1 \end{bmatrix} \tag{12}$$

The elastic stiffness matrix will then contain off-diagonal coupling terms reflecting the difference between the two rotation points:

$$\boldsymbol{D}_{z^p_{LRP}} = \begin{bmatrix} k^e_v & 0 & 0 \\ 0 & k^e_h & -(z^p_{LRP} - z^e_{LRP})\, k^e_h \\ 0 & -(z^p_{LRP} - z^e_{LRP})\, k^e_h & k^e_\theta + (z^p_{LRP} - z^e_{LRP})^2\, k^e_h \end{bmatrix} \tag{13}$$

The depths, z^e_{LRP} and z^p_{LRP}refer to the distance from the *SFI*.

5.2. Macro-element input

The modifications presented in Section 5.1 may seem like an overcomplication, as the only change from a mathematical point of view is an elastic stiffness matrix with off-diagonal terms. However, the concept with two defined rotational points is justified by the user input interface. The macro-element relies on input based FEA reflecting the

Table 1
Required input to the macro-element accounting for foundation flexibility.

Input	Purpose/usage
The depth to the internal load reference points at initial mobilization, z^e_{LRP} and at failure, z^p_{LRP}. The centre of rotation can be computed by equation (5) when a moment load is applied at the SFI.	Determine the cross coupling between horizontal and moment load
The response curves from three analyses as tabulated data: 1. Vertical load vs. vertical displacement ($V - u_v$) for pure vertical loading at the SFI. 2. Horizontal load vs. horizontal displacement ($H - u_h$) for pure horizontal translation at the SFI. The load and displacement should be extracted from the SFI. However, the analysis should apply a rigid lid and restrict it from rotation such that the response reflect only translation response. 3. Moment vs. rotation response (M - u_θ) for pure moment loading at the SFI at the SFI.	The three curves define the anisotropic hardening (stiffness).
Number of yield surfaces, N.	The number defines the discretization of the piece-wise linear hardening.

conditions of the problem at hand. The advantage of this approach is the increased accuracy compared to hardcoded parameters and closed form solutions, as explained in (Page et al., 2017; Skau et al., 2017; K. S. S. Skau et al., 2018a). By applying a moment load at the *SFI*, the ratio $u_{h,SFI}/u_\theta$ (Equation (6)) can be plotted as function of the mobilization. The depths, z^e_{LRP} and z^p_{LRP}can then be determined as depth at initial mobilization and the depth at failure.

The complete list of required input is given in Table 1. Fig. 6 illustrates these input parameters. The z^e_{LRP} parameter is the only additional required parameter compared to the input requirements of the macro-element as presented in (K. S. S. Skau et al., 2018b).

6. Comparison with FEA

The implementation of caisson flexibility into the macro-element was verified by comparing FEA results with the response computed by the macro-element. The case considered represents a realistic design situation such that conclusions and observations are relevant for practical design.

6.1. Case properties

6.1.1. Site condition and geotechnical properties

A soil profile comprising a homogenous uniform clay with constant shear strength of $s_u^C = 150$ kPa with depth was considered in this study (s_u^C refers to undrained triaxial compression strength). The NGI-ADP soil model (Grimstad et al., 2012) was used in the analyses. The model is a total-stress-based model with an anisotropic shear strength. The nonlinear shear-stress – shear-strain response starts with G_{max} and depends further on the applied stress path according to the anisotropic formulation.

The soil input was defined to reflect the stress-strain response of 2-way symmetric cyclic loaded clay described according to the NGI Drammen clay database with an over consolidation ratio, OCR = 4 and a number of equivalent cycles of $N_{eq} = 10$. Andersen (2015) and K. S. Skau et al. (2017) provide more information on the details of the NGI-procedure for interpretation of the effect of cyclic loading on soils and the extraction of corresponding stress-strain curves. Table 2 gives the used soil parameters for the NGI-ADP model. The seabed inside and outside the skirts were modelled with a 0.25 m difference due to soil plug heave during installation.

6.1.2. Caisson geometry and structural properties

An 8 m diameter caisson with 6 m deep skirts was considered in the study. The caisson was modelled in detail to ensure a realistic structural behaviour. Fig. 8 shows a finite element model of the structural details of the caisson. The steel was assumed to have a Young's modulus $E = 2.1E8$ kPa. A grout thickness of 0.25 m was assumed based on experience from full scale installations. The soil plug was assumed incompressible and the grout stiffness was assumed to be 9 times the initial soil stiffness (i.e. $G_{grout} = 9 \cdot G_{soil,max}$). The loads were applied at a

Table 2
Input parameter values for the NGI-ADP model.

Parameter	Value	Parameter explanation
s_u^A (kPa)	150	Triaxial compression shear strength
S_u^P/s_u^A	0.56	Ratio between shear strength from triaxial extension and triaxial compression
S_u^{DSS}/s_u^A	0.74	Ratio between shear strength from direct simple and triaxial compression
τ_0 (kPa)	0.0	Initial shear mobilization
G_{ur}/s_u^A	500	Ratio between initial stiffness and triaxial compression shear strength
γ_f^C (%)	2.5	Shear strain at failure from triaxial compression
γ_f^E (%)	3.6	Shear strain at failure from triaxial extension
γ_f^{DSS} (%)	3.4	Shear strain at failure from direct simple shear

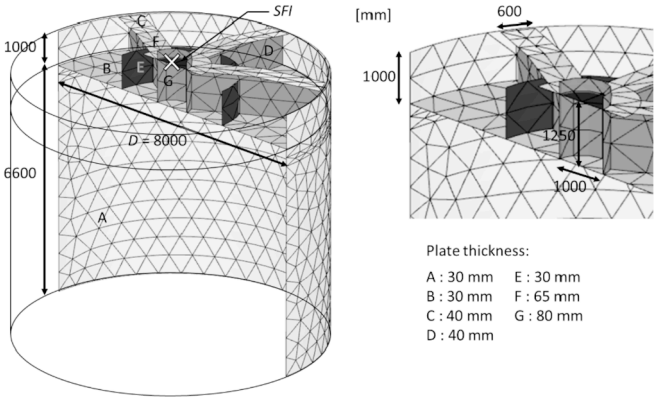

Fig. 8. Structural configuration of caisson foundation.

SFI, 1.25 m above the lid plate (see Fig. 8). The caisson flexibility is occasionally evaluated by the so called relative flexibility (Cox et al., 2014):

$$Et/DG_{soil,max} \tag{14}$$

where t is the skirt thickness. The considered geometry has a relative flexibility of 10.5, in line with the two prototype mono-caisson OWTs listed in (Cox et al., 2014). However, it should be mentioned that the relative flexibility do not provide any information about the lid flexibility.

6.2. Finite element model

The commercially available *Finite Element* (FE) software PLAXIS 3D AE (PLAXIS, 2015) was used in the numerical study. The soil was modelled with 10-noded tetrahedral elements, and the structural parts with 6-noded quadratic triangular plate elements. Interface elements were used between structure and soil as additional mesh refinement to avoid stress concentration near singular points. However, no strength reduction was applied in the interface. Only in-plane loading was

Table 3
Initial stiffness computed by FEA compared to initial stiffness based on closed form solutions by Doherty and Deeks (2003).

	Vertical stiffness (kN/m)	Rotational stiffness (kNm/rad)	Horizontal stiffness (kN/m)
FEA	3.04E + 06	3.56E + 07	2.72E + 06
Doherty and Deeks (2003)	3.00E + 06	3.64E + 07	2.70E + 06

considered, and to reduce the computational cost, only half of the physical problem was modelled utilizing symmetry. The side boundaries were located 60 m from the foundation centre, and the bottom boundary 60 m below seabed. Fig. 8 shows the FE-model. The mesh discretization was found to be acceptable based on a sensitivity study where the moment–rotation response was compared with a model with finer mesh. Compared to the refined model, the model used in the study gave an overshoot of less than 10% at failure, but the response curves coincided for loads up to 80% mobilization, which is the load level of greatest interest in this study. The FEA was also validated by comparing the computed initial stiffnesses assuming a rigid caisson, against the closed form solutions proposed by Doherty and Deeks (2003). The initial stiffness under vertical loading, moment loading and horizontal translation (no rotation) were computed by both methods. The stiffnesses, given in Table 3, are in very good agreement (less than 3% difference).

6.3. FEA results for macro-element input

The FEA results were first used as input to the macro-element, as specified in Table 1. The input load - displacement responses for a flexible caisson foundation are shown in Fig. 10. To get more information of the effects of caisson flexibility, analyses were performed assuming three different caisson flexibilities:

1. Fully flexible caisson
2. Fully rigid caisson
3. Rigid lid and flexible skirts

The results, included in Fig. 10, shows the additional displacement from the caisson deflection modes. The vertical stiffness of the rigid and flexible caisson agree fairly well with the observations in Shonberg et al. (2017). This confirms the relevance of the case for a caisson foundation in a jacket configuration. The moment stiffness is dramatically changed when the caisson flexibility is included. This increase in rotational flexibly is likely to be too large for e.g. a mono-tower configuration, where the rotational stiffness is important. However, the exact rotational stiffness was considered secondary here since the purpose was to demonstrate that the macro-element accuracy was sufficient compared to FEA results. A stiffer caisson would have given response more similar to rigid foundation response which already has been considered and verified in (K. S. S. Skau et al., 2018a,b). The horizontal stiffness is little affected by the skirt flexibility. This is not a general conclusion, since only one case is considered. However, the limited effected agree with the findings by (Doherty et al., 2005), and the skirt wall thickness of 30 mm cannot be reduced much without making the skirts insufficient for installation. Further differences will be discussed in more detail in section 7.

The effect of the flexible lid affects the z_{LRP} as expected from the discussion on deflection modes. Fig. 10 gives the z_{LRP}, determined by equation (6), for the three foundation flexibilities as function of global mobilization. The *LRP* for the flexible caisson is more load dependent than the *LRP* for the rigid foundation. The normalization parameter h^* is the sum of skirt length, h, and the distance from the lid to the *SFI* ($h^* = h + 1.25$ m).

Table 4
Macro-element input parameters.

Parameter	z^e_{LRP} (m)	z^p_{LRP} (m)	N
Value	0.8	4.7	15

6.4. Macro-element input

The response of the fully flexible caisson in Fig. 10 was used as the uniaxial macro-element input. The two macro-element input depths, representing the elastic and plastic load reference point, were based on the results in Fig. 10: $z^e_{LRP} = 0.8$ m and $z^e_{LRP} = 4.7$ m. The hardening function was discretized by $N = 15$ yield surfaces.

7. Results from the comparison

Fig. 11 shows the response of the three input curves computed by FEA compared to those produced by the macro-element. As expected, the macro-element reproduces the input curves. The macro-element was then compared with results from FEA when subjected to more general load paths. Table 4 summarizes these paths which were specified to challenge the model's accuracy in the *MH*-load plane. The load and displacement components (M, H, u_h, u_θ) are most affected by the foundation flexibility and they are also strongly coupled. Fig. 12a compares the resultant values, that means the magnitude of the load and displacement vectors ($|\boldsymbol{F}|$ and $|\boldsymbol{u}|$), and Fig. 12b compares the displacement components u_h and $u_\theta D/2$. Both figures show results at the *SFI*. The agreement between FEA and macro-element response is very good(see Fig. 13) (see Table 5).

7.1. Effect on soil displacements around the foundation

The FEA-results were also used to examine the foundation behaviour during loading, in particular how the flexibility affects the response in the soil around the foundation. The flexibility effects were examined at a load level less than 20% of the failure load which was considered relevant for OWTs.

7.2. Response to vertical loading

The response to vertical loading is shown in Fig. 9a as load-displacement curves. The perfectly rigid foundation and the foundation with rigid lid and flexible skirt show a nearly coinciding response. The fully flexible caisson is significantly softer, especially at low mobilization levels. The difference in foundation response of the three cases becomes negligible close to failure.

The displacement in the soil was studied in more detail for a vertical load of $V = 10\,000$ kN. At this mobilization level, Fig. 10a indicates that the caisson flexibility contributes to approximately 55% of the total flexibility of the foundation. This is comparable to the contributions seen in the measurements in Fig. 3. Fig. 14 shows contours of vertical displacements in the soil. The vertical displacements are also shown for three cross-sections at different depths in Fig. 15. Horizontal dotted lines indicate the depths in Fig. 14. The figures show, that the vertical

Table 5
General load paths applied to foundation at foundation-structure interface (FSI).

	V (MN)	H (MN)	2M/D (MN)
Path 1	0	55.8	−65.7
Path 2	0	21.4	0
Path 3	24	24.2	0
Path 4	160	0	10
Path 5	140	−40	7.5

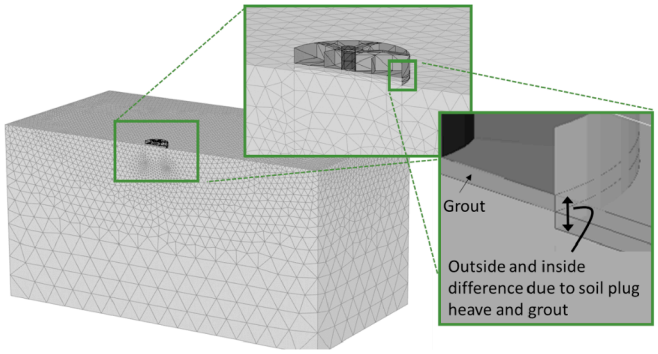

Fig. 9. FE-model of soil and foundation.

displacement in the soil approaches gets less influenced by the caisson flexibility with depth. At skirt tip level the vertical displacements coincide. Since the soil is incompressible, it is clear that the soil has to deform in the radial direction forcing the skirt periphery to increase (not shown herein but observed in FEA). The observation means that the lid deflection interact with the nonlinear soil reactions and the skirt flexibility as assumed in macro-element modification.

7.3. Response to moment loading

The response to moment loading is shown in Fig. 10b as load – displacement curves. In line with the vertical load case, the perfectly rigid caisson and the foundation with rigid base and flexible skirt show a nearly coinciding response. The fully flexible caisson is significantly softer, especially at low mobilization levels. The vertical displacements in the soil below the foundation were examined at a moment load, $2M/D = 5000$ kN. Fig. 16 shows shadings of vertical displacements in the soil. The vertical displacements are also shown for three depths in Fig. 16. Dotted horizontal lines indicate these depths in Fig. 15. The reducing influence of the caisson flexibility on vertical displacement with depth is similar to the pattern seen for pure vertical loading. Despite a large difference close to the lid, the three foundation cases give almost identical vertical displacements at skirt tip.

7.4. Response to horizontal loading

The response to horizontal loading was assessed in combination with a rotational fixity of the entire lid to isolate the effect of skirt deflection. Fig. 10c shows the horizontal response for the perfectly rigid caisson and the perfectly rigid lid and flexible skirt. The analyses of the caisson with flexible lid was not included in the comparison since the additional flexibility from lid bending is significantly larger than the skirt deflection. The effect of lid bending is already considered in Section 7.2. The limited difference between the two curves in Fig. 10c suggests that the global response is relatively little affected by the skirt flexibility. For the ratio of skirt thickness and caisson diameter in the present case (Doherty et al., 2005), suggests a reduced horizontal stiffness of 10–20%. However, the numbers are not directly comparable since the study presented in Doherty et al. (2005) allowed the caisson to rotate in combination with the translation. The horizontal displacements in the soil are examined for a horizontal load of $H = 8000$ kN. Fig. 18 shows contours of horizontal displacements. The horizontal displacements are also shown along three vertical lines, each at a different distance from the foundation centre in Fig. 19. Dotted vertical lines indicate the location of these lines in Fig. 18. The difference in the horizontal displacements from the two analyses with the two caisson flexibility assumptions reduces with depth and with the horizontal distance away from the foundation. The differences are negligible 5 m from the foundation centre (1 m from the skirt periphery) (see Fig. 17).

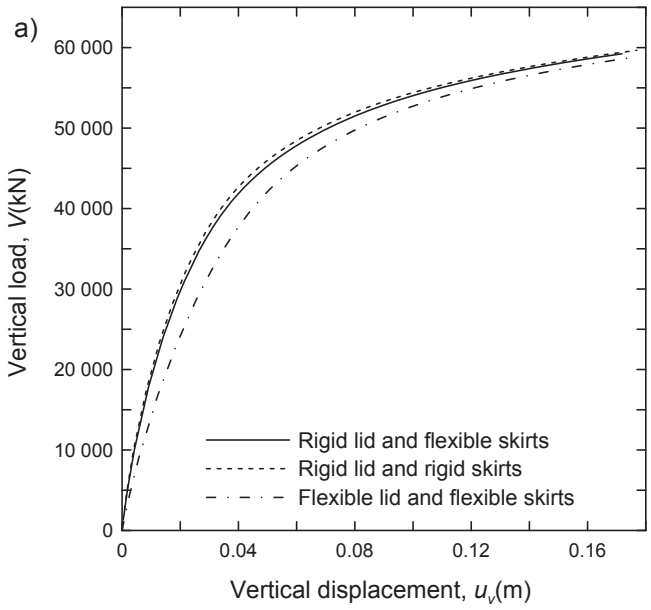

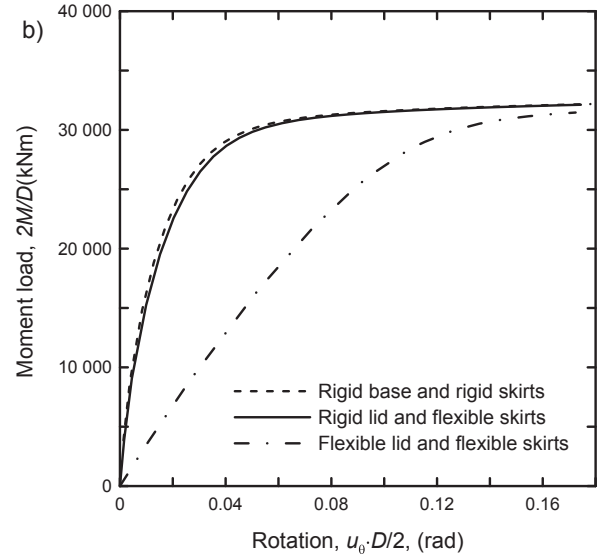

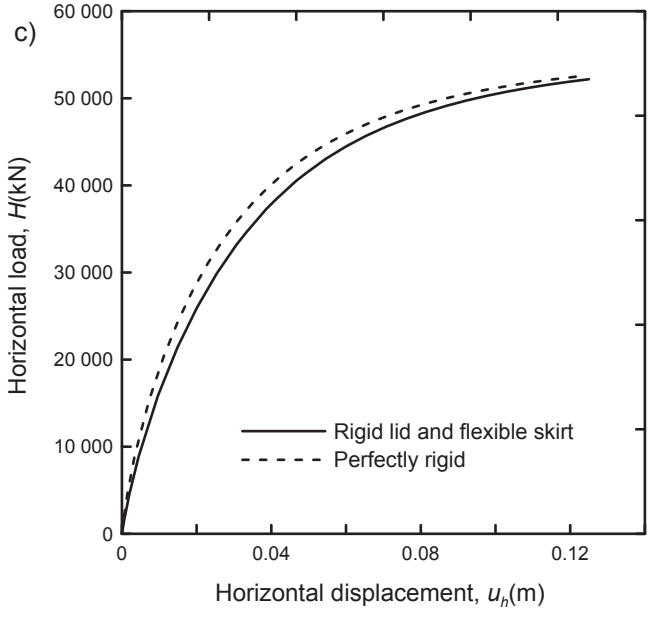

(caption on next page)

Fig. 10. Foundation response a) Vertical load – vertical displacement b) Moment load - rotation c) Horizontal load – horizontal displacement.

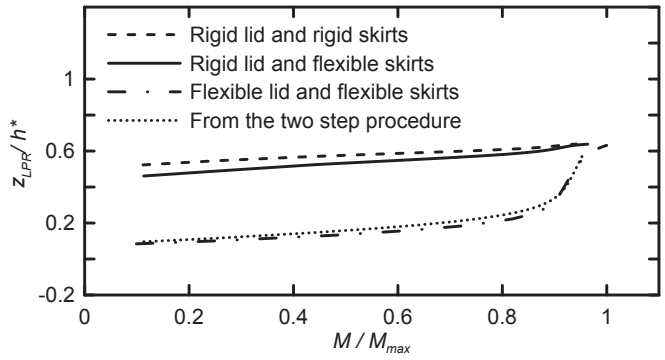

Fig. 11. Depth to the load reference point, zLRP/h*.

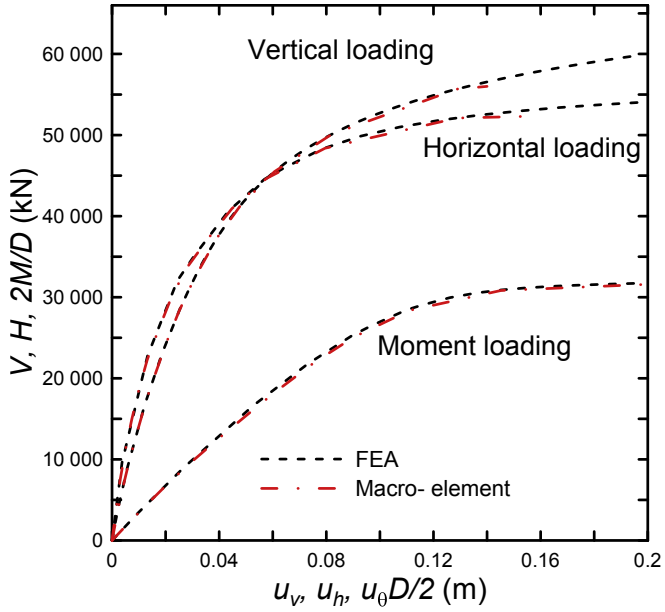

Fig. 12. Uniaxial curves for the fully flexible caisson.

8. Discussion on structure-foundation interface and design work flow

The case considered in this example used the interface between structure and foundation (*SFI*) right above the lid (Figs. 4 and 9). This is reasonable for a final design. The situation may be different in a design, where the caisson configuration may be optimized by an iterative process and structural details such as skirt thickness and lid configurations are modified based the latest set of analyses. Since these modifications may influence the caisson flexibility, the foundation response has to be updated to reflect the modifications. If the caisson diameter and skirt depth are kept constant, it may be convenient to model the caisson flexibility by a linear elastic super-element linking the support structure and the macro-element assuming a rigid caisson. The super-element properties can then be updated without touching the (rigid) macro-element input parameters. This super-element stiffness can be recognized as the $\boldsymbol{D}_{flex\ bucket}$ stiffness matrix in Equation (9). Section 8.1 propose a simplified procedure to approximate the elastic caisson flexibility super-element stiffness. The purpose of the procedure is to streamline the design work flow.

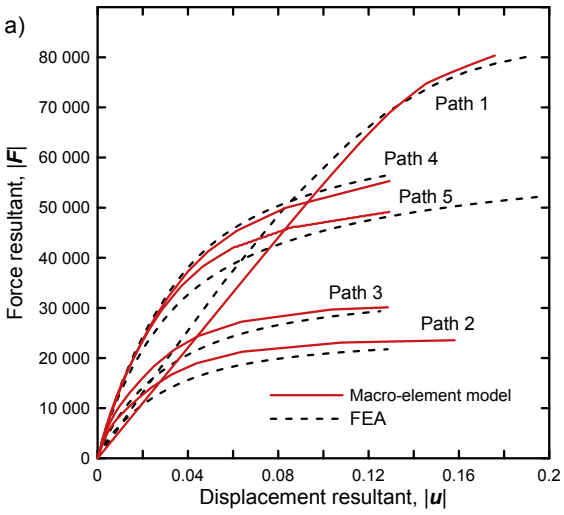

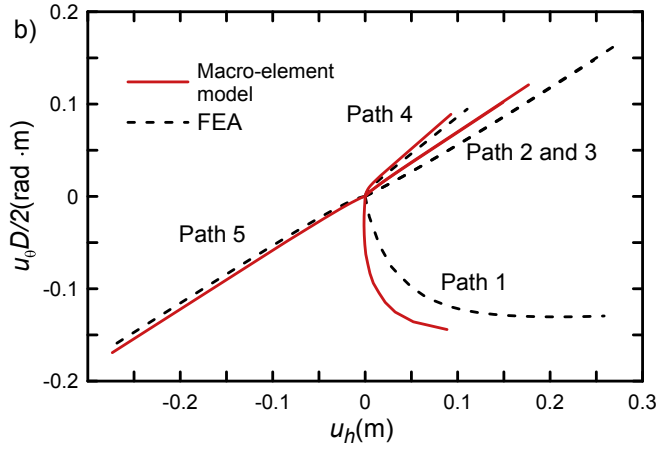

Fig. 13. Foundation response computed by FEA and macro element. a) Resultant response, b) displacement components u_h and u_θ.

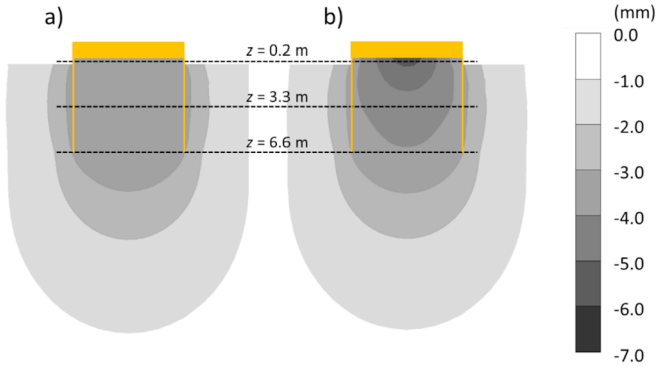

Fig. 14. Vertical displacements in the soil under vertical loading a) Rigid foundation b) Flexible caisson.

8.1. Computation of flexible caisson response by sub-modelling

The observations from the FEA results suggest that the lid deflection affects the soil mainly inside the skirts. The zone influenced by the skirt deflection during horizontal loading, could not be defined with equally clear boundaries. However, the displacements reduced rapidly outside the skirts and became a very small fraction of the total displacements. These observations allow for a simplification in the computation of

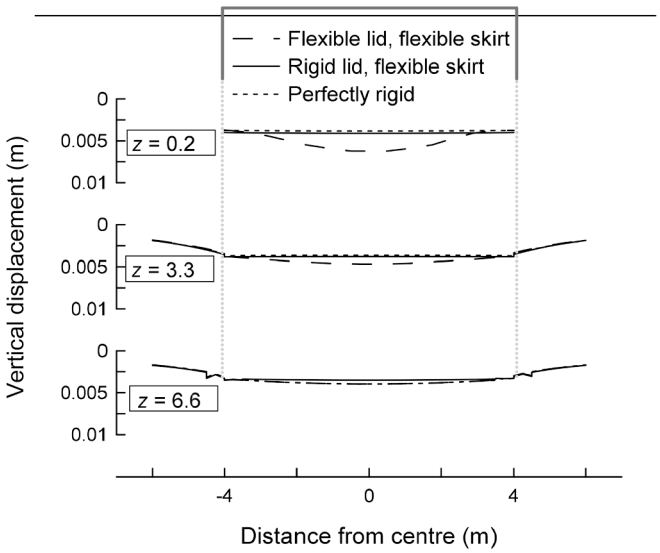

Fig. 15. Vertical deformation in three depth under vertical loading.

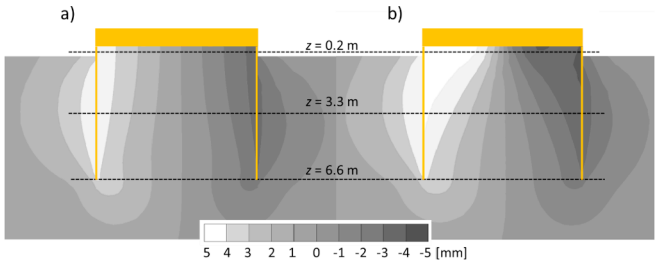

Fig. 16. Vertical displacements in the soil under moment loading a) Rigid foundation b) Flexible caisson.

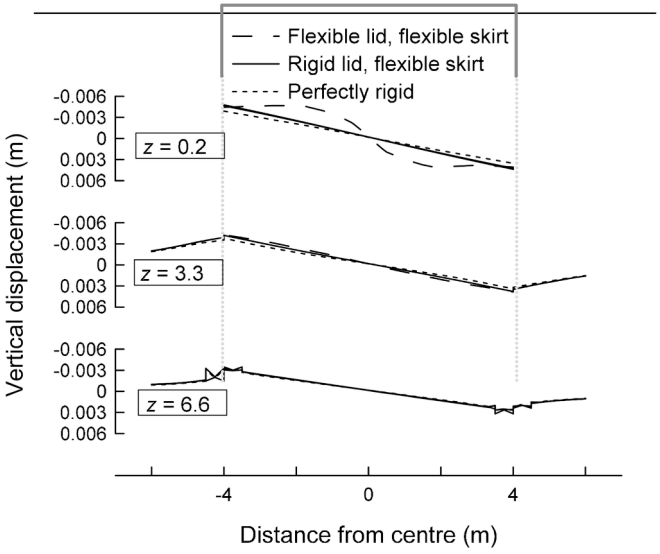

Fig. 17. Vertical deformations in three depth below foundation under moment load.

foundation response in the three uniaxial directions as required for macro-element input. The authors propose a *two step* procedure where the uniaxial responses are derived by superposition of results from two models:

1) A global model of a rigid caisson and the complete far field soil domain.

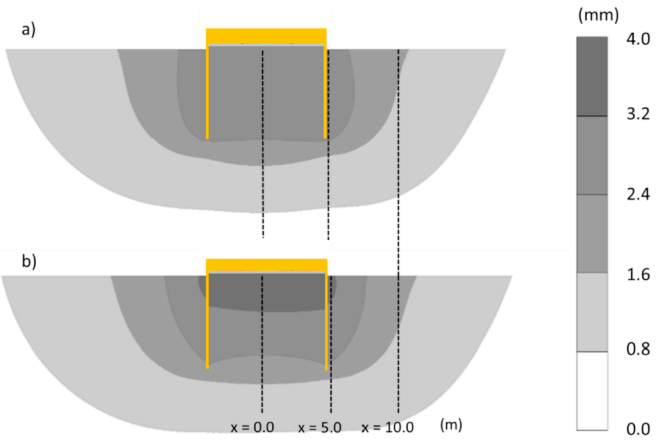

Fig. 18. Horizontal displacement in the soil under horizontal loading a) Rigid foundation, b) Flexible skirts and rigid lid.

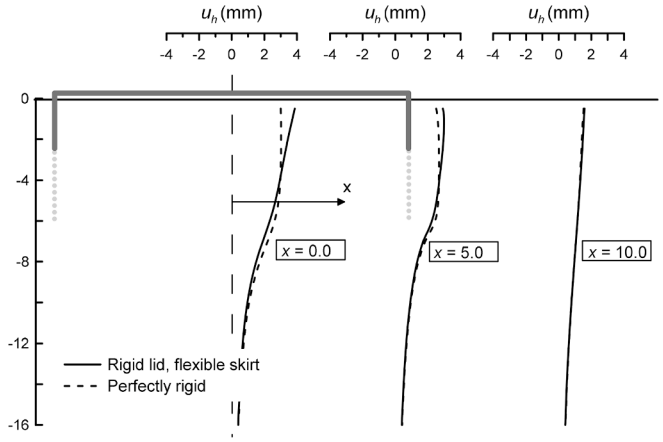

Fig. 19. Horizontal displacement in three vertical cross section under horizontal loading.

2) A sub-model of the caisson with the real flexibility.

The term *global model* and *sub-model* will be used to denote the two models. The *global foundation model* is similar to the already presented FE-model in Fig. 9, with a rigid caisson model. This model will not be described in more detail in this section. The foundation response computed by this model does not change as long as the foundation diameter and skirt is constant.

The sub-models should reflect the additional flexibility in the three uniaxial directions. The models are smaller, thus faster to run and the effect of caisson flexibility modifications can be effectively updated in a design loop. Note that the three deformation modes in Fig. 6 give displacements in exactly the three uniaxial directions. Because the deflection mode depends on the applied load, different boundary conditions are required in the analyses of the three load situations. The *sub-models* are shown in Fig. 20 and the modelling recommendations are described below.

a) Vertical deflection of the lid

The soil outside the skirts and below the skirt tip can be ignored. Vertical fixity is required at skirt tip level. The skirts should not be restricted horizontally, such that they can displace radially (hoop-deformations).

b) Bending deflection of the lid

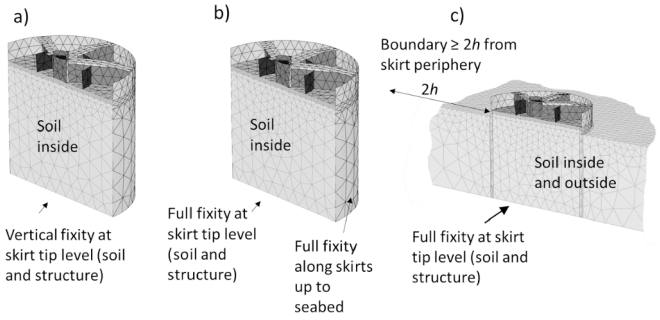

Fig. 20. Illustration of the sub-models and required boundary conditions. a) Vertical lid deflection, b) Bending lid deflection load, c) skirt deflection.

The soil outside the skirts and below the skirt tip can be ignored. The model considering lid bending deflection displaces the soil inside the skirts. Thus, radial fixity can be applied along the skirts to prevent rotation of the whole foundation. The soil is fixed from vertical displacement at skirt tip level.

c) Deflection of the skirt.

It was found that the soil outside the skirts had to be included to obtain sufficient accuracy. The side boundaries should be located at least 2 h away from the skirt periphery. Horizontal fixity should be applied to the skirt tip.

The validity of this procedure was evaluated by comparing the response determined by superposition and the response computed directly in FEA with a flexible caisson model. Fig. 21 shows the comparison in uniaxial directions. The agreement is good. The soil was represented by the NGI-ADP model in all the *sub-models*. The soil model is incompressible, and the compressibility should be accurately modelled in these analyses as it is likely to affect the lid support as shown by Doherty et al. (2005) for flexible skirts and discussed for large gravity based concrete caisson structures in Skau et al. (2010). However, Fig. 21 shows that the foundation flexibility was almost linear for all load directions. This suggest that a linear elastic soil modelled could have been used in the sub-models for these conditions. However, this assumption should be checked for the specific case considered.

9. Conclusions

The effect of caisson flexibility was implemented in an existing macro-element by modifying the elastic stiffness matrix and the required input parameters. The modifications were based on an

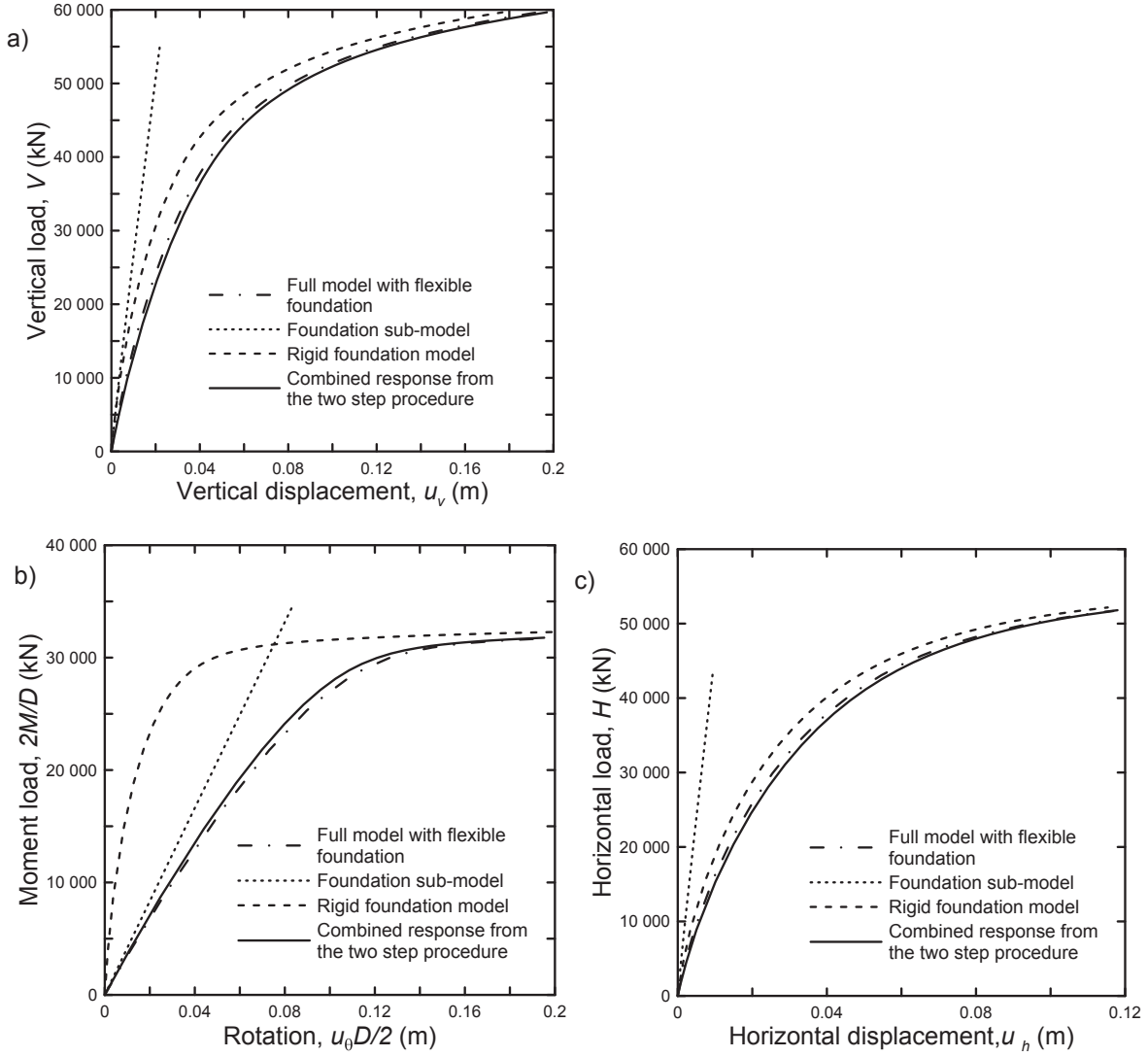

Fig. 21. Comparison of the foundation response based on superposition and the full FEA with flexible caisson. a) Vertical load, b) Moment load c) Horizontal load with lid bending restricted.

assessment of possible caisson deflection modes and the consequences for a foundation model formulation. The additional flexibility reduces the overall stiffness and influences the coupling between the moment and the horizontal load. The response computed by the macro-element agreed well with the response computed in FEA. The FEA results suggest that the lid flexibility is more important than the skirt flexibility for the overall foundation stiffness.

The agreement between the FEA and the macro-element response is important not only for this specific macro-element, but for modelling of caisson flexibility in general. The agreement suggests that the foundation flexibility can be approximated with sufficient accuracy by an elastic correction to the response of a rigid foundation. This is an extension of the proposed series coupled spring model for vertical stiffness, and implies that the foundation flexibility alternatively can be modelled as linear elastic super-element between the structure and a macro-element representing rigid foundation response. This observation made it possible to propose a sub-model procedure to establish the foundation response. The procedure super impose the uniaxial response computed for a rigid foundation in a global FE-model and the response from the caisson flexibility, computed in a smaller sub-model. This may streamline the design process. However, a more extensive study is required to ensure the validity for different foundation geometries, foundation flexibilities and soil conditions.

The recent full scale measurement data, the theoretical assessment and numerical results presented herein, clearly show that caisson flexibility has to be addressed in design of caissons for OWT-structures.

Acknowledgement

The financial support by the Norwegian Geotechnical Institute, the Norwegian Research Council and the industrial partners Statoil, Vattenfall and Statkraft through project Reducing cost of offshore wind by integrated structural and geotechnical design (REDWIN), Grant No. 243984, is gratefully acknowledged.

References

Andersen, K., 2015. Cyclic soil parameters for offshore foundation design. In: Proceedings of Frontiers in Offshore Geotechnics (ISFOG) III. CRC Press, Oslo, Norway, pp. 5–82.

Andersen, K.H., Murff, J.D., Randolph, M.F., Clukey, E.C., Erbrich, C.T., Jostad, H.P., Hansen, B., Aubeny, C., Sharma, P., Supachawarote, C., 2005. Suction anchors for deepwater applications. Keynote paper. In: International Symposium on Frontiers in Offshore Geotechnics, Proceedings. Perth, Australia, pp. 3–30.

Andresen, L., Petter Jostad, H., Andersen, K., 2011. Finite element analyses applied in design of foundations and anchors for offshore structures. Int. J. GeoMech. 11, 417–430. https://doi.org/10.1061/(ASCE)GM.1943-5622.0000020.

Bienen, B., Byrne, B.W., Houlsby, G.T., Cassidy, M.J., 2006. Investigating six-degree-of-freedom loading of shallow foundations on sand. Geotechnique 56, 367–379. https://doi.org/10.1680/geot.2006.56.6.367.

Bordón, J.D.R., Aznárez, J.J., Maeso, O.F., 2016. Three-dimensional BE-FE Model of bucket foundations in poroelastic soils. In: Proceedings of the VII European Congress on Computational Methods in Applied Sciences and Engineering (ECCOMAS Congress 2016). Athens, Greece, pp. 8725–8738. https://doi.org/10.7712/100016.2445.7331.

Butterfield, R., Ticof, J., 1979. The use of physical models in design. In: 7th European Conf. On Soil Mechanics and Foundation Engineering (ECSMF), 4. Brighton, UK, pp. 259–261.

Bye, A., Erbrich, C., Rognlien, B.T.T., 1995a. Geotechnical design of bucket foundations. In: The Offshore Technology Conference, . https://doi.org/10.4043/7793-MS.

Bye, A., Erbrich, C., Rognlien, B.T.T., 1995b. Geotechnical design of bucket foundations. In: The Offshore Technology Conference, . https://doi.org/10.4043/7793-MS.

Byrne, B.W., 2000. Investigations of Suction Caissons in Dense Sand. Oxford University.

Cassidy, M.J., Martin, C.M., Houlsby, G.T., 2004. Development and application of force resultant models describing jack-up foundation behaviour. Mar. Struct. 17, 165–193. https://doi.org/10.1016/j.marstruc.2004.08.002.

Cox, J.A., O'Loughlin, C.D., Cassidy, M., Bhattacharya, S., Gaudin, C., Bienen, B., 2014. Centrifuge study on the cyclic performance of caissons in sand. Int. J. Phys. Model. Geotech. 14, 99–115. https://doi.org/10.1680/ijpmg.14.00016.

Cremer, C., Pecker, A., Davenne, L., 2001. Cyclic macro-element for soil-structure interaction: material and geometrical non-linearities. Int. J. Numer. Anal. Methods GeoMech. 25, 1257–1284. https://doi.org/10.1002/nag.175.

Dekker, M.J., 2014. The Modelling of Suction Caisson Foundations for Multi-footed Structures. Master Thesis. Norwegian University of Science and Technology (NTNU).

DNV, 2016. Support Structures for Wind Turbines, DNVGL-ST-0126.

Doherty, J.P., Deeks, A.J., 2003. Elastic response of circular footings embedded in a non-homogeneous half-space. Geotechnique 53, 703–714. https://doi.org/10.1680/geot.2003.53.8.703.

Doherty, J.P., Houlsby, G.T., Deeks, A.J., 2005. Stiffness of flexible caisson foundations embedded in nonhomogeneous elastic soil. J. Geotech. Geoenviron. Eng. 131, 1498–1508. https://doi.org/10.1061/(ASCE)1090-0241(2005)131:12(1498.

Gottardi, G., Butterfield, R., 1993. On the bearing capacity of surface footings on sand under general planar loads. Soils Found. 33, 68–79. https://doi.org/10.3208/sandf1972.33.3_68.

Gourvenec, S., Barnett, S., 2011. Undrained failure envelope for skirted foundations under general loading. Geotechnique 61, 263–270. https://doi.org/10.1680/geot.9.T.027.

Grange, S., Kotronis, P., Mazars, J., 2009. A macro-element to simulate 3D soil–structure interaction considering plasticity and uplift. Int. J. Solid Struct. 46, 3651–3663. https://doi.org/10.1016/j.ijsolstr.2009.06.015.

Grimstad, G., Andresen, L., Jostad, H.P., 2012. NGI-ADP: anisotropic shear strength model for clay. Int. J. Numer. Anal. Methods GeoMech. 36, 483–497. https://doi.org/10.1002/nag.1016.

Grimstad, G., Rønningen, J.A., Nøst, H.A., 2014. Use of IWAN models for modelling anisotropic and cyclic behaviour of clays. In: Proceeding of Nummerical Methods in Geootechnical Engneering Volume I. Trondheim, Norway, pp. 49–55.

Houlsby, G.T., 2016. Interactions in offshore foundation design. Geotechnique 66, 791–825. https://doi.org/10.1680/jgeot.15.RL.001.

Houlsby, G.T., Byrne, B.W., 2000. Suction caisson foundations for offshore wind turbines and anemometer masts. Wind Eng. 24, 249–255. https://doi.org/10.1260/0309524001495611.

Houlsby, G.T., Cassidy, M.J., Einav, I., 2005. A generalised Winkler model for the behaviour of shallow foundations. Geotechnique 55, 449–460. https://doi.org/10.1680/geot.2005.55.6.449.

Ibsen, L., Barari, A., Larsen, K., 2014. Adaptive plasticity model for bucket foundations. J. Eng. Mech. 140, 361–373. https://doi.org/10.1061/(ASCE)EM.1943-7889.0000633.

Iwan, W.D., 1967. On a class of models for the yielding behavior of continuous and composite systems. J. Appl. Mech. 34, 612–617. https://doi.org/10.1115/1.3607751.

Jalbi, S., Shadlou, M., Bhattacharya, S., 2018. Impedance functions for rigid skirted caissons supporting offshore wind turbines. Ocean Eng. 150, 21–35. https://doi.org/10.1016/j.oceaneng.2017.12.040.

Jostad, H.P., Nadim, F., Andersen, K.H., 1994. A computational model for fixity of spud cans on stiff clay. 7th Int. Conf. Behav. offshore Struct. 1, 151–172.

Koiter, W.T., 1953. Stress-strain relations, uniqueness and variational theorems for elastic-plastic materials with a singular yield surface. Q. Appl. Math. 11, 350–354. https://doi.org/10.1090/qam/59769.

Liingaard, M., Andersen, L., Ibsen, L.B., 2007. Impedance of flexible suction caissons. Earthq. Eng. Struct. Dynam. 36, 2249–2271. https://doi.org/10.1002/eqe.737.

Martin, C.M., 1994. Physical and Numerical Modelling of Offshore Foundations under Combined Loads, PhD Thesis. University of Oxford.

Martin, C.M., Houlsby, G.T., 2001. Combined loading of spudcan foundations on clay: numerical modelling. Geotechnique 51, 687–699. https://doi.org/10.1680/geot.2001.51.8.687.

Nguyen-Sy, L., Houlsby, G.T., 2005. The theoretical modelling of a suction caisson foundation using hyperplasticity theory. In: International Symposium on Frontiers in Offshore Geotechnics, 19-21 September. Taylor and Francis, Perth, Australia, pp. 417–423.

Nova, R., Montrasio, L., 1991. Settlements of shallow foundations on sand. Geotechnique 41, 243–256. https://doi.org/10.1680/geot.1991.41.2.243.

Offshore Wind, 2017. GWEC Global Wind 2016 Report.

Page, A.M., Skau, K.S., Jostad, H.P., Eiksund, G.R., 2017. A New Foundation Model for Integrated Analyses of Monopile-based Offshore Wind Turbine.

PLAXIS, 2015. PLAXIS 3D EA. www.plaxis.com.

Prager, W., 1955. The theory of plasticity: a survey of recent achievements. Arch. Proc. Inst. Mech. Eng. 169, 41–57. 1847-1982 (vols 1-196. https://doi.org/10.1243/PIME_PROC_1955_169_015_02.

Prisco, C.G. di, Wood, D.M., 2012. Mechanical Behaviour of Soils under Environmentallly-induced Cyclic Loads. Springer Science & Business Media.

Roscoe, K.H., Schofield, A.N., 1956. The stability of short pier foundations in sand: discussion. Br. Weld. J. 343–354.

Shonberg, A., Harte, M., Aghakouchak, A., Pachecco, M., Cameron, S.D., Lingaard, M., 2017. Suction bucket jackets for offshore wind turbines: applications from in situ observations. In: Proceedings of the 19th International Conferance on Soil Mechanics and Geotechnical Engineering. Soul.

Skau, K., Kayna, A.M., Jostad, H.P., 2010. 3D FE SSI analyses of the Troll A platform. In: Geoteknikkdagen, pp. 38.

Skau, K.S., Chen, Y., Jostad, H.P., 2018a. A numerical study of capacity and stiffness of circular skirted foundations in clay subjected to combined static and cyclic general loading. Geotechnique 68, 205–220. https://doi.org/10.1680/jgeot.16.P.092.

Skau, K.S., Kaynia, A.M., Page, A.M., Løvholt, F., Norén-Cosgriff, K., Sturm, H., Jostad, H.P., Nygard, T.A., Andersen, H.S., Eiksund, G., Havmøller, O., Strøm, P., Eichler, D., 2017. REDWIN – REDucing cost in offshore WINd by intregrated structural and geotechnical design. In: Geteoteknikkdagen. Oslo, pp. 38.1–38.17.

Skau, K.S.S., Grimstad, G., Page, A.M.M., Eiksund, G.R.R., Jostad, H.P.P., 2018b. A macro-element for integrated time domain analyses representing bucket foundations for offshore wind turbines. Mar. Struct. 59, 158–178. https://doi.org/10.1016/j.marstruc.2018.01.011.

Sturm, H., 2017. Design aspects of suction caissons for offshore wind turbine foundations. In: Proceedings of the 19th International Conferance on Soil Mechanics and Geotechnical Engineering. Seoul, Korea.

Suryasentana, S., Byrne, B.W., Burd, H.J., Shonberg, A., 2017. A simplified model for the

stiffness of suctuion caisson foundations under 6 DOF loading. In: SUT OSIG 8th International Conferance. London, UK.
Tjelta, T., 1995. Geotechnical experience from the installation of the europipe jacket with bucket foundations. In: The Offshore Technology Conference (OTC). The Offshore Technology Conference, Houston, Texas. https://doi.org/10.4043/7795-MS.
Tjelta, T.I., 2001. Suction piles: their position and application today. In: The Eleventh International Offshore and Polar Engineering Conference. Stavanger, Norway.
Vabbersgaard, L., Bo, L., Andersen, L., Ibsen, L., Liingaard, M., 2009. Lumped-parameter model of a bucket foundation. In: Computational Geomechanics : COMGEO I: Proceedings of the 1st International Symposium on Computational Geomechanics (COMGEO I). Juan -les- Pins, France, pp. 731–742.
Ziegler, H., 1959. A modification to Prager's hardening rule. Q. Appl. Math. 17, 55–65.